The impact of range-dependent sediment properties on the acoustic field in 2-D shallow water environments

Jason D. Sagers
Applied Research Laboratories at The University of Texas at Austin
Environmental Science Laboratory
Austin, TX 78758
phone: (512) 835-3195 fax: (512) 490-4225 email: sagers@arlut.utexas.edu

Award Number: N00014-10-1-0650

LONG-TERM GOALS

The goal of this research is to understand the effects of range-dependent sediment properties on the acoustic field in 2-D shallow water environments. This information, in part, is required to solve the statistical inference problem in inhomogeneous shallow water environments.

OBJECTIVES

The spatio-temporal variability of the water column needs to be properly accounted for while looking for the effect of range-dependent sediment properties on the acoustic field. The objective of the current work is to create a high-fidelity model of the water column along a single propagation track for the Shallow Water 2006 (SW06) experiment. The water column model is constructed from oceanographic data measured at moorings located along the acoustic propagation track. The water column model describes oceanographic features on several space-time scales, including those ranging from frontal boundaries to nonlinear internal waves. The purpose of the water column model is to reduce the mismatch between measured and modeled acoustic data so that other propagation effects, such as range-dependent sediment properties can be investigated in the future.

APPROACH

The main goal of the work is to investigate the impact of range-dependent sediment properties on the acoustic field in the SW06 environment. However, during an analysis of acoustic data in the region of interest, it was observed that the passage of internal waves caused significant temporal fluctuations in the acoustic data. The temporal fluctuations on a single hydrophone ranged anywhere from a few dB to more than 25 dB. This observation is common to many shallow water regions of the ocean.[1,2,3,4,5] When trying to extract information about range-dependent sediment properties from acoustic data in shallow water waveguides, it is important to separate, insofar as possible, the part of the acoustic field that depends on spatio-temporal fluctuations of the water column from the part of the acoustic field that depends on range-dependent sediment properties.

Report Documentation Page

Form Approved
OMB No. 0704-0188

1. REPORT DATE	2. REPORT TYPE	3. DATES COVERED
2012	**N/A**	**-**

4. TITLE AND SUBTITLE	5a. CONTRACT NUMBER
The impact of range-dependent sediment properties on the acoustic field in 2-Dshallow water environments	5b. GRANT NUMBER
	5c. PROGRAM ELEMENT NUMBER
6. AUTHOR(S)	5d. PROJECT NUMBER
	5e. TASK NUMBER
	5f. WORK UNIT NUMBER
7. PERFORMING ORGANIZATION NAME(S) AND ADDRESS(ES) **Applied Research Laboratories at The University of Texas at Austin Environmental Science Laboratory Austin, TX 78758**	8. PERFORMING ORGANIZATION REPORT NUMBER
9. SPONSORING/MONITORING AGENCY NAME(S) AND ADDRESS(ES)	10. SPONSOR/MONITOR'S ACRONYM(S)
	11. SPONSOR/MONITOR'S REPORT NUMBER(S)

12. DISTRIBUTION/AVAILABILITY STATEMENT
Approved for public release, distribution unlimited

13. SUPPLEMENTARY NOTES
The original document contains color images.

14. ABSTRACT

15. SUBJECT TERMS

16. SECURITY CLASSIFICATION OF:			17. LIMITATION OF ABSTRACT	18. NUMBER OF PAGES	19a. NAME OF RESPONSIBLE PERSON
a. REPORT	b. ABSTRACT	c. THIS PAGE			
unclassified	**unclassified**	**unclassified**	**SAR**	**6**	

The approach taken here was to develop a data-driven water column model of the SW06 region and link it to an acoustic propagation model. The acoustic predictions from the model are then compared with measured acoustic data from the SW06 experiment to determine the utility of the water column model, and the extent to which it can be used to predict fluctuations in received acoustic intensity. The water column model encompasses a 30 km track between SW47 and SW54 as shown in Fig. 1.

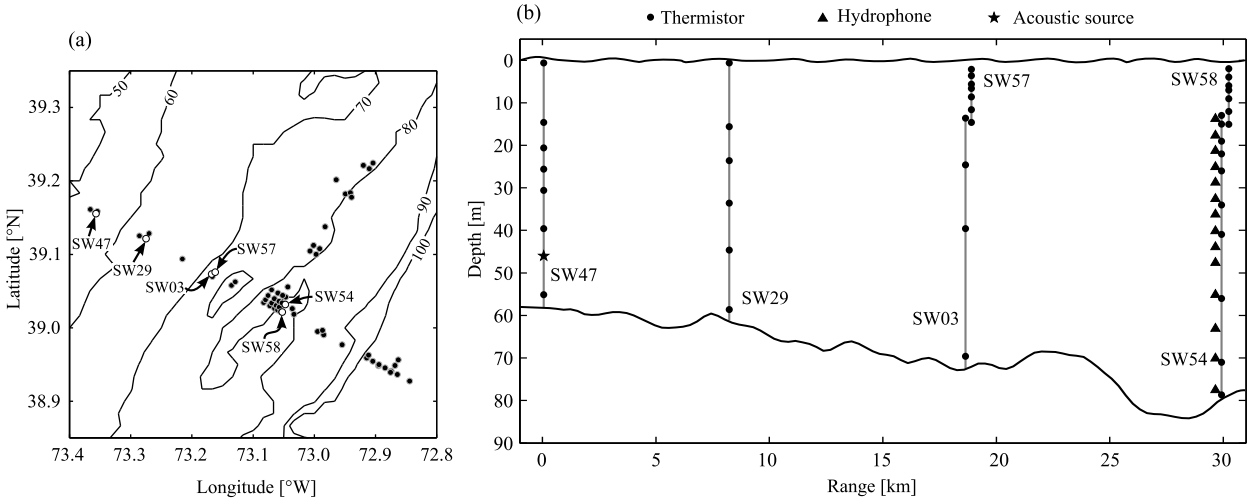

Figure 1: (a) Map of the SW06 experimental region with overlaid bathymetric contours and mooring locations shown by dots. The focus of this work is a region defined by the line connecting SW47 and SW54. (b) Location of thermistors, hydrophones, and the acoustic source in the range-depth plane between SW47 and SW54.

A 224 Hz acoustic source was moored at SW47 and acoustic intensity was received on a vertical line array (VLA) of hydrophones at SW54. The received acoustic intensity as a function of time was integrated over the vertical aperture to create depth-integrated intensity $I_z(t)$. Because $I_z(t)$ captures the vertical distribution of energy in the water column, fluctuations in this quantity reflect changes in the net attenuation experienced by the acoustic wave as it undergoes modal scattering by the internal wave field. Depth-integrated intensity was chosen as the acoustic metric for the comparison between measured and modeled data. The usefulness of the water column model will be assessed by its ability to predict the acoustic depth-integrated intensity received on SW54.

The key to creating a useful water column sound speed profile from thermistor data measured at discrete spatial locations is the method by which the data are processed and interpolated in both space and time. Figure 2 shows the processing steps employed to create a spatio-temporal water column sound speed profile from salinity and temperature recordings at multiple discrete spatial positions. This process is discussed in detail in Chs. 3 and 4 of Ref. 6. One important feature of the process shown in Fig. 2 and discussed in Ref. 6 is that any number of oceanographic moorings can be incorporated into the oceanographic model. If more than one oceanographic mooring is included in the processing, then the internal wave packet will evolve as a function of space and time. For this reason, this method was called the evolutionary propagated thermistor string (EPTS) method. If only a single oceanographic mooring is included, then the oceanographic model resembles the propagated thermistor string (PTS) method used in prior work.[7,8]

The modeled water column sound speed profile $c(r,z,t)$ was linked to an acoustic propagation model to

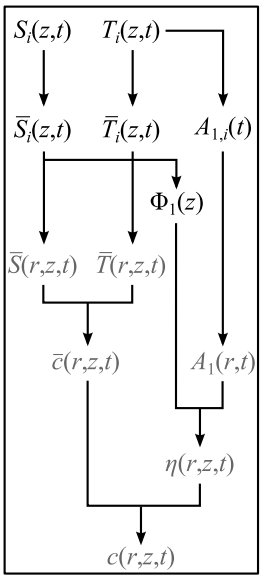

Sym.	Quantity	Units
S	salinity	[ppt]
T	temperature	[°C]
c	sound speed	[m/s]
A_1	IW mode 1 amp.	[m]
Φ_1	IW mode 1 shape	
η	IW displacement	[m]
i	SW47, SW29, SW03, SW54	
$\overline{\ }$	the overbar means that a 24-hr moving-average filter has been applied	

Figure 2: Data flow diagram showing how temperature and salinity data from discrete spatial locations are processed to produce a water column sound speed profile.

predict the acoustic field at the SW54 VLA. The range-dependent acoustic model (RAM) was selected for this task. Benchmarking against a more accurate two-way coupled mode algorithm showed that the RAM model possessed sufficient accuracy to compute the acoustic field in the presence of nonlinear internal waves. This is important because the computational efficiency of RAM made it possible to predict the acoustic field every 15 seconds for more than 3 weeks of the SW06 experiment.

Finally, measured and modeled $I_z(t)$ were compared at the SW54 VLA to assess the usefulness of the oceanographic model for predicting acoustic intensity fluctuations.

WORK COMPLETED

The work completed includes the following items:

1. Creating the EPTS method for computing $c(r,z,t)$ from measured oceanographic data at discrete mooring positions.
2. Linking the water column model to RAM, and computing depth-integrated acoustic intensity at the SW54 VLA.
3. Processing acoustic data at the SW54 VLA over 21 days of the experiment.
4. Comparing the modeled acoustic data to the measured acoustic data to validate the water column model.
5. Investigating correlations between the amplitude of the internal wave field and the statistics of acoustic intensity in both measured and modeled data.

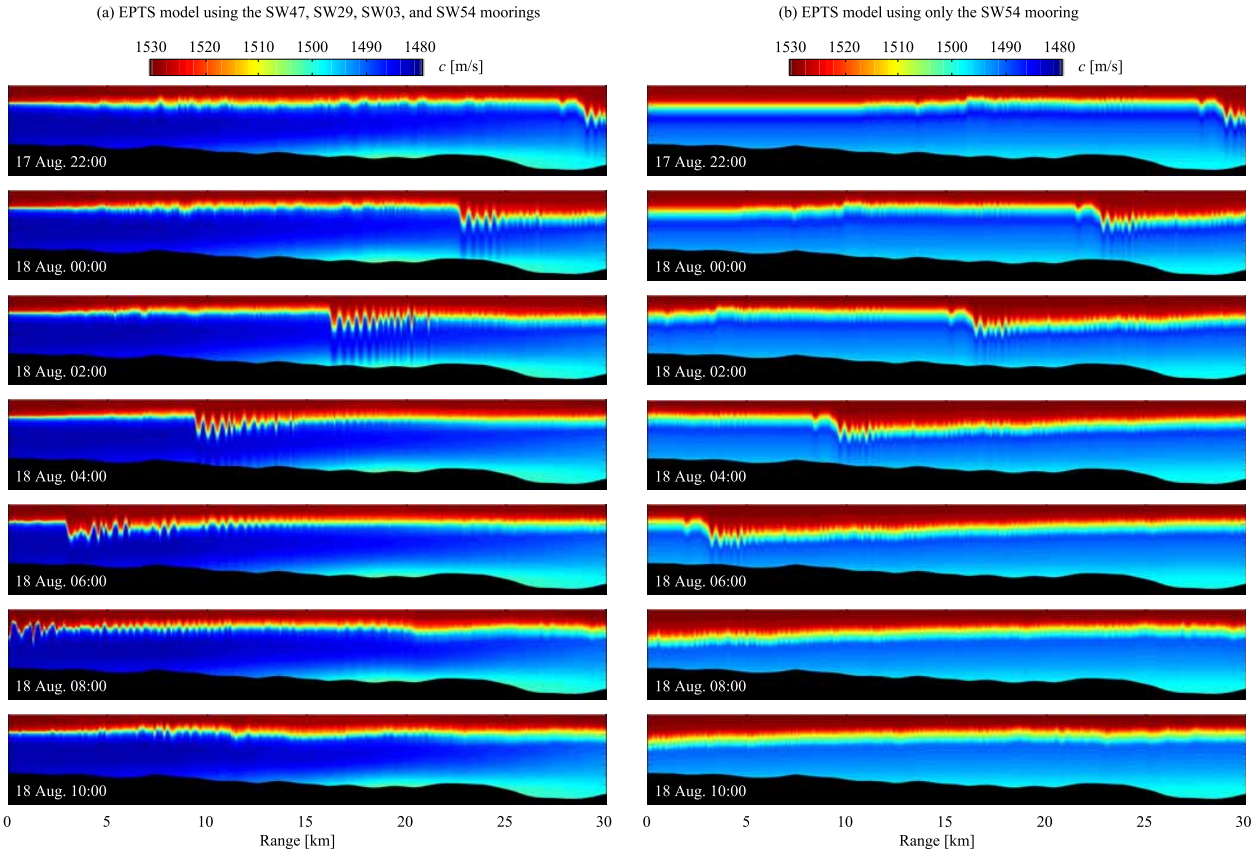

Figure 3: Snapshots shown every 2 hrs of $c(r,z,t)$ generated by the EPTS model for internal wave event 6 using (a) four and (b) one mooring in the EPTS model.

RESULTS

Snapshots of $c(r,z,t)$, shown every 2 hrs during internal wave event 6 (17 August 22:00 through 18 August 10:00), are shown in Fig. 3. Data from four oceanographic moorings (SW47, SW29, SW03, and SW54) were used to create the profiles shown Fig. 3(a), while data from a single mooring (SW54) were used to create the profiles shown in Fig. 3(b). Figure 3(a) contains a range-dependent background sound speed profile $\bar{c}(r,z,t)$ and shows the evolution of the internal wave packet as it propagates up the continental shelf. In contrast, Fig. 3(b) possesses a range-independent $\bar{c}(r,z,t)$ and the internal wave packet translates but does not evolve as it propagates.

While Figs. 3(a) and (b) appear to have much in common, the differences in $c(r,z,t)$ can dramatically affect the ability to accurately predict the acoustic field. This is demonstrated in Fig. 4(a) through (c) which show $I_z(t)$ from measured data, modeled EPTS data using four moorings, and modeled EPTS data using one mooring, respectively.

In general, $I_z(t)$ from Fig. 4(c) is not as accurate as $I_z(t)$ from Fig. 4(b) when predicting the measured data. The model errors come in at least two types. The first type of error is visible between 24 to 29 August, where $I_z(t)$ in Fig. 4(c) is 5 to 10 dB below the measured value. This particular error results from the construction of a range-independent $\bar{c}(z,t)$ from only $\bar{T}_{\mathrm{SW54}}(z,t)$ and $\bar{S}_{\mathrm{SW54}}(z,t)$. Between approximately 24 to 29 August the shelf-break front moved inshore of the SW54 mooring bringing warmer, saltier water near SW54. This oceanographic front was physically localized near SW54 and

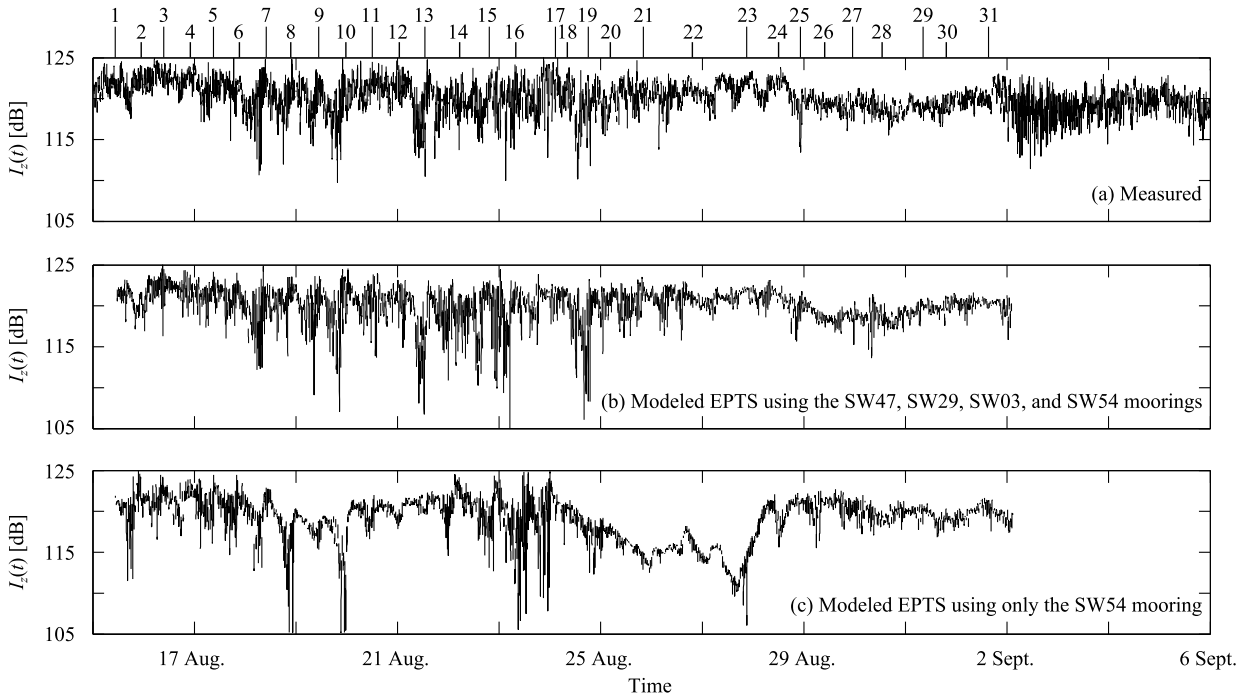

Figure 4: Comparison between (a) measured, (b) EPTS modeled (four moorings), and (c) EPTS modeled (one mooring) $I_z(t)$ with internal wave event numbers shown at the top.

did not represent the background water column conditions over the entire 30 km track. However, the sound speed reconstruction used to generate the acoustic data shown in Fig. 4(c) has no information input about this range-dependent feature and reconstructs the entire water column sound speed profile from local conditions. The net result is acoustic predictions with large errors in the time-averaged value of $I_z(t)$.

The second type of error in $I_z(t)$ for Fig. 4(c) occurs in predictions for shorter time scales. The details of the short-time fluctuations in Fig. 4(c) do not reflect those appearing in Fig. 4(a). This type of error results from the construction of the internal wave field from a single thermistor string. Thus, the details of the internal wave field are not as accurate as they are for the EPTS model when using multiple moorings. For example, an inspection of events 12 to 13 and 18 to 19 in Fig. 4 shows that the single-mooring model does not capture the approximately 10 dB fluctuations present in both Fig. 4(a) and (b). Another example of this type of error is visible for event 16 for which the single-mooring model produces fluctuations approximately 10 dB too large. The change in the structure of the internal wave field as it propagates shoreward appears to significantly affect the accuracy of the acoustic prediction on short time scales.

It was shown that large fluctuations in acoustic intensity can be accurately predicted by the EPTS model when data from multiple moorings are included. The ability to improve the comparison between measured and modeled acoustic data is important for solving the range-dependent geoacoustic inverse problem. If the water column is not properly accounted for, then errors in the acoustic prediction arising from errors in the modeled $c(r,z,t)$ will be translated to the geoacoustic inverse or inference problem in the form of model error.

IMPACT/APPLICATIONS

The impact of this research is to demonstrate how accurately the acoustic field can be predicted in the presence of internal waves for long propagation distances in shallow water. Applications of this research range from sonar prediction problems to accounting for a spatio-temporally varying water column in inversion and statistical inference problems.

TRANSITIONS

The primary transition for this project is a methodology for reconstructing a modeled sound speed profile $c(r,z,t)$ from multiple oceanographic moorings in a continental shelf environment.

RELATED PROJECTS

None.

REFERENCES

[1] J. Zhou, X. Zhang, and P. H. Rogers, "Resonant interaction of sound wave with internal solitons in the coastal zone", J. Acoust. Soc. Am. **90**, 2042–2054 (1991).

[2] J. Apel, M. Badiey, C. Chiu, S. Finette, R. Headrick, J. Kemp, J. Lynch, A. Newhall, M. Orr, B. Pasewark, D. Tielbuerger, A. Turgut, K. Von Der Heydt, and S. Wolf, "An overview of the 1995 SWARM shallow-water internal wave acoustic scattering experiment", IEEE J. Oceanic Eng. **22**, 465–500 (1997).

[3] R. H. Headrick, J. F. Lynch, J. N. Kemp, A. E. Newhall, K. von der Heydt, J. Apel, M. Badiey, C. S. Chiu, S. Finette, M. Orr, B. Pasewark, A. Turgot, S. Wolf, and D. Tielbuerger, "Acoustic normal mode fluctuation statistics in the 1995 SWARM internal wave scattering experiment", J. Acoust. Soc. Am. **107**, 201–220 (2000).

[4] T. F. Duda, J. F. Lynch, A. E. Newhall, L. Wu, and C. Chiu, "Fluctuation of 400-Hz sound intensity in the 2001 ASIAEX South China Sea experiment", IEEE J. Oceanic Eng. **29**, 1264–1279 (2004).

[5] J. R. Apel, L. A. Ostrovsky, Y. A. Stepanyants, and J. F. Lynch, "Internal solitons in the ocean and their effect on underwater sound", J. Acoust. Soc. Am. **121**, 695–722 (2007).

[6] J. D. Sagers, "Predicting acoustic intensity fluctuations induced by nonlinear internal waves in a shallow water waveguide", Ph.D. thesis, The University of Texas at Austin (2012).

[7] R. H. Headrick, "Analysis of internal wave induced mode coupling effects on the 1995 SWARM experiment acoustic transmissons", Ph.D. thesis, MIT (1997), ch. 3.

[8] R. H. Headrick, J. F. Lynch, J. N. Kemp, A. E. Newhall, K. von der Heydt, J. Apel, M. Badiey, C. S. Chiu, S. Finette, M. Orr, B. Pasewark, A. Turgot, S. Wolf, and D. Tielbuerger, "Modeling mode arrivals in the 1995 SWARM experiment acoustic transmissions", J. Acoust. Soc. Am. **107**, 221–236 (2000).